Heliyon 10 (2024) e27585

Contents lists available at ScienceDirect

Heliyon

journal homepage: www.cell.com/heliyon

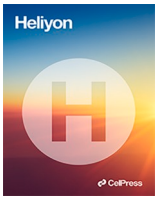

Research article

Construction of carbon nanospheres: A rational design based on BS-12 @ LiCl

Bingxuan Du [a], Haichao Li [a,*], Conglin Zhang [a], Qingsong Ji [b]

[a] Qinghai Nationalities University, Institute of Resource Chemistry of Qinghai, Xining 810007, PR China
[b] Institute of Chemical Industry of Forest Products, Chinese Academy of Forestry, National Engineering Laboratory for Biomass Chemical Utilization, Nanjing 210042, PR China

ARTICLE INFO

Keywords:
Carbon nanosphere
Self-assembly
Separator
Tunableness

ABSTRACT

Nanocarbons have potential applications in almost all areas of materials science. While we have appreciated the various discoveries and applications of many nanocarbons, we recognize that the field remains challenging in terms of tunability. In this research, we report a new strategy for the self-assembly of surfactant @ salt from the concept of carbon nanostructure design, and introduce the concept of "separator". On the one hand, it allows the core and shell to be formed in one step. On the other hand, it allows the ordered aggregates to remain in their original shape under thermal action. The surface morphology, degree of graphitization, elemental composition and surface chemical state, formation mechanism, and specific luminescent properties of carbon nanomaterials were investigated. TEM reveals that (dodecyldimethyl betaine) BS-12 @ LiCl carbon nanospheres with tunable size (from 55 nm to 70 nm) can be successfully synthesized. Raman and XRD show that the structure of carbon nanospheres has some defects and disordered carbon. XPS and FTIR analyses indicate that the defects present in the carbon nanosphere structure are related to the N and O elements. The detailed growth mechanism shows that the micelle structure in the system can be well adjusted by changing the concentration of surfactant. PL research demonstrates that the synthesized carbon nanospheres have UV luminescent properties. Most importantly, the method can be further developed into a general strategy for self-assembly using a variety of surfactants and "separators" as promising candidates for future practical applications of nanocarbon materials.

1. Introduction

Nanocarbon materials have received much attention due to their unique structural design and various promising applications, especially in organic electronics and biology [1]. However, numerous studies have shown that the application performance of carbon nanomaterials depends on their ability to be tailored at the nanoscale [2,3]. Among the fascinating nanocarbon materials, carbon nanospheres have been extensively researched in the past decade due to their unique properties, such as good thermal stability and excellent biocompatibility [4]. Compared to other carbon nanomaterials, the spherical morphology as well as the small diameter of carbon nanospheres make them more suitable for use as electrode materials in energy storage systems [5]. This is mainly attributed to the fact that the spherical morphology guarantees high packing densities, while the small diameter implies short transport distances

* Corresponding author.
E-mail address: lihaichao@vip.163.com (H. Li).

https://doi.org/10.1016/j.heliyon.2024.e27585
Received 5 January 2024; Received in revised form 2 March 2024; Accepted 4 March 2024
Available online 8 March 2024

[5]. Based on the above reasons, the synthesis of carbon nanospheres has attracted increasing attention. To date, various strategies have been proposed for the preparation of carbon nanospheres with tunable dimensions and specific optical properties. The synthesis order can be broadly classified into bottom-up (pre-core-post-shell) and top-down (pre-shell-post-core) approaches [6–10]. In the bottom-up approach, the core carbon nanoparticles are first produced. In the bottom-up approach, the core carbon nanoparticles are first produced, and then the surface of the formed cores is encapsulated in shells using either a soft or hard template approach [11]. In the top-down approach, the shells are first prepared, and then the core carbon nanoparticles are introduced into the hollow shells [11]. In the last 10–15 years, scientists have made exciting developments using these two synthetic routes [1]. However, most of the research on nanocarbon has shown that the emergence of its different morphologies and sizes led to the discovery of functions and applications that were not initially anticipated [1]. Therefore, we believe that the establishment of new methods and techniques for the synthesis of tunable nanocarbon structures has a great impetus for future breakthroughs in the design and application of carbon nanostructures.

In this work, we report a surfactant @ salt self-assembly method for the synthesis of tunable-size and UV-emitting carbon nanospheres. The method involves the establishment of a (dodecyldimethyl betaine) BS-12 @ LiCl micelle system. Notably, we propose the use of concentrated salt (LiCl) as a "separator". Its primary function is to provide a unique environment of separation and confinement for the micelles. Importantly, this approach allowed us to adjust the size of the carbon nanospheres by controlling the concentrations of the surfactant (BS-12). The micellar system is driven by shear flow to direct the self-assembly of BS-12 @ LiCl precursors, and spherical micelles are encapsulated in LiCl as the self-assembly proceeds further. Finally, after carbonization, the separating layers can be further exfoliated to form on-demand carbon nanospheres. Obviously, the present synthetic strategy does not belong to the pre-core−post-shell or pre-shell−post-core methodologies [11]. The core and shell are formed in one step during the self-assembly process, which further demonstrates the novelty and simplicity of our synthesis strategy. The article is based on the idea of nanostructure design. Our focus is on proposing a new synthetic strategy, the surfactant @ salt self-assembly strategy, and introducing the concept of "separator". To the best of our knowledge, this new strategy and concept have not been reported yet. In recent years, novel methodologies for synthesizing nanomaterials have been developed. For example, F. Dehghani et al. produced graphite-based nanocomposites by deposition-precipitation techniques [12]. It should be mentioned that this synthesis strategy requires the precursor to be synthesized in advance. A. Mirzaei et al. proposed the fabrication of G nanosheets by means of a pulse current sintering (PCS) process with fullerene clusters as source materials [13]. Notably, the synthesis method is highly equipment dependent and requires preparation under vacuum and high pressure. Often, these newly developed methods are not as facile (no advance preparation, no cumbersome processes), efficient (no complex synthesis environments), and low-cost (NaCl can be recovered) as the methods developed in this work. Additionally, since many types of surfactants and inorganic salts exist for combination, we believe that a variety of carbon nanostructures with different morphologies can be designed and synthesized in the future using the surfactant @ salt self-assembly strategy. This efficient, facile, low-cost, and environmentally friendly method provides new insights into synthesizing carbon nanomaterials.

2. Experimental section

2.1. Materials

All commercially available reagents were analytical grade and ready for use without further purification. Ultrapure water was used in all experiments. NaCl and dodecyl dimethyl betaine (BS-12) were purchased from Aladdin Biochemical Technology (Shanghai) Co. Reagents (99 % analytically graded) were used as received without furthe refinement.

2.2. Synthesis

With BS-12 as the carbon source and LiCl as the separator, the self-assembly strategy of separating first and then carbonizing was adopted to synthesize the carbon nanospheres of tunable size. First, BS-12 at different concentrations (1 CMC, 5 CMC and 10 CMC) was stirred at a slow speed (300 rpm). During the stirring process, the shear flow drives the micelles gradually to spherical shape for dynamic self-assembly and buries the hydrophobic alkyl chains inside the micelles. LiCl (120 g) was then added continuously in slow heating (60 °C) until it was fully crystallized and encapsulated in the aggregates. As the separator penetrates from aggregate to aggregate, the aggregates were eventually encapsulated in the LiCl crystalline layer. Spherical precursors with a core-shell structure were formed from the inside out. After separation, the precursors were charred at 500 °C for 1 h, and the "shells" were removed with a large amount of deionized water, leaving a series of carbon nanospheres with specific sizes.

2.3. Methods

TEM images were obtained with a JEM-2100F transmission electron microscope (JEOL, Japan) at 200 KV. Raman spectra were measured by an InVia Reflex laser microscope confocal Raman spectrometer (Renishaw, UK). An argon-ion laser was used as the excitation light source, and the excitation wavelength was set to $\lambda = 532$ nm. The spectral range of the acquisition was from 100 to 3000 cm^{-1}. The crystalline structure parameters of the samples were determined using a D/MAX-B type X-ray diffractometer from RIKEN, Japan. Cu target radiation ($\lambda = 0.154056$ nm) and scanned the sample at a scanning speed of 4 (°)/min in the range of $2\theta = 15°–60°$. X-ray photoelectron spectroscopy (XPS) was measured on a Thermo ESCALAB 250XI (Thermo Fisher Scientific, US) system. Fourier transform infrared spectra (FTIR) were recorded on a Nicolet FT170SX spectrometer (Thermo Fisher Scientific, US) in the range of 500–4000 cm^{-1} with a resolution of 2 cm^{-1}. The fluorescence spectra were recorded by an F-4600 fluorescence spectrometer (Hitachi, Japan). The emission spectra were recorded in the range of 250~440 nm at the excitation wavelengths of 280 nm, 300 nm,

320 nm, and 340 nm, respectively.

3. Results and discussion

Here, we propose a simple general strategy of separation followed by carbonization to prepare tunable carbon nanospheres. The synthesis includes the establishment of BS-12 @ LiCl carbon nanospheres with BS-12 as the core and LiCl as the shell, and the proposed use of concentrated salt as the "separator". Briefly, the first key idea is the dynamic self-assembly of micelles into BS-12 @ LiCl precursors with a core-shell structure driven by shear flow. Obviously, this is different from the traditional pre-core-post-shell or pre-shell-post-core approach [11]. The synthesis method introduces LiCl, which allows the core and shell to be formed in one step. The second key idea is to maintain the aggregated morphology under thermal action to form stable BS-12 @ LiCl carbon nanospheres. This also relies on the concept of "separators" that we have proposed. Specifically, LiCl plays an important role in the non-collapse and deformation of micelles during the carbonization process. The retention of this structure is caused by the high-temperature resistance of the crystalline layers and by the constraining effect. The method of preparing BS-12 @ LiCl carbon nanospheres and the results of their surface morphology are shown in Fig. 1.

In the preparation process, we believe that salts have an important role in separating and limiting. Since direct carbonization of BS-12 after self-assembly in aqueous solution usually leads to severe aggregation, uncontrolled carbide surface morphology, and poor dispersion. We introduce salt as a "separator", which easily penetrates into the micelle-to-micelle space and clads the micelle during the stirring process, forming a crystalline layer framework. It is worth noting that salt can be recycled. In addition, due to its high temperature resistance, salt can act as a barrier to prevent ordered aggregates from aggregating during high-temperature carbonization. Thus, its limiting effect allows the original shape and size of the precursor to be well preserved. More importantly, the rational design and controlled synthesis of carbon nanostructures with well-defined dimensions and morphologies has been a long-sought goal [14]. We can induce micelles to change from small to large size by simply changing the CMC value of the surfactant in a concentrated salt system. This makes it possible to precisely control the size of carbon nanospheres.

The morphology and dimensions of BS-12 @ LiCl precursors are shown in the TEM images of Fig. 1b, c, d. Under different concentration conditions, LiCl can penetrate well into the micelle voids and form a clear and dispersed core-shell structure. However, incomplete penetration of LiCl into the micelles leads to the formation of aggregated structures between the aggregates. In addition, the images show that the 1 CMC and 10 CMC precursors have an overall spherical morphology, but the individual shapes are slightly different. It is noteworthy that the spherical morphology of the precursors is deformed to some extent as the surfactant concentration increases to 5 CMC. Among these different nanocarbon structures, the high integrity of the internal structure of the charred precursors is of great interest to us (Fig. 1e, f, g). This can be attributed to the fact that the introduction of LiCl can work well as a protective layer to maintain the spherical structure. After de-shelling, the diameter of 1 CMC sample is significantly reduced from 83 to 100 nm to about 55 nm. However, the diameter of 10 CMC sample is reduced from 100 to 130 nm to about 70 nm under the same charring conditions. The change in particle size during charring, which we believe may not be just a simple size contraction of BS-12 within the BS-12 @ LiCl core due to pyrolysis. LiCl creates a closed environment on BS-12, and the high-temperature resistant structure of LiCl reduces the

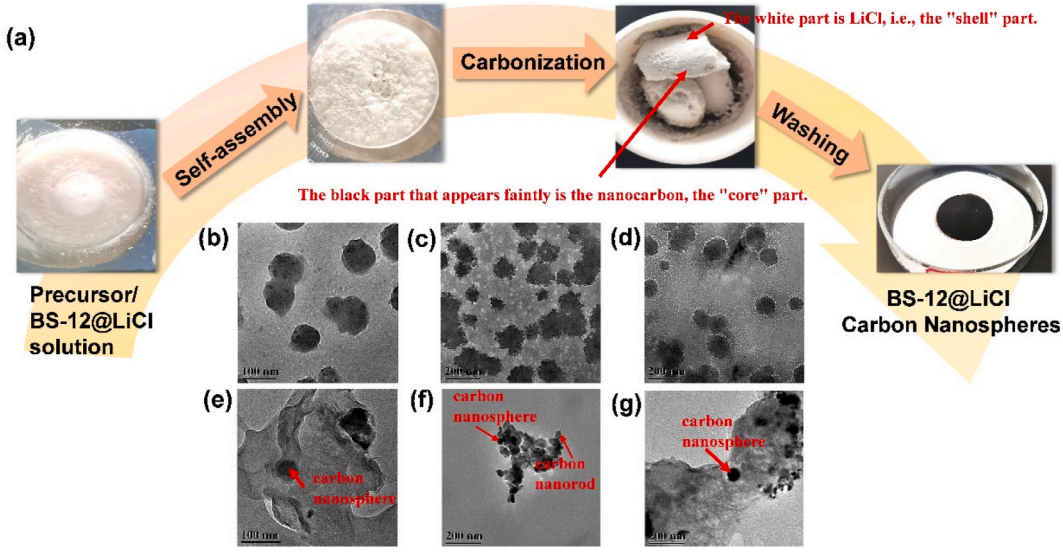

Fig. 1. Synthesis of carbon nanospheres using surfactant @ salt. (a) The formation process of BS-12 @ LiCl carbon nanospheres with shell-core structure. (b) Representative TEM image showing precursors of 1 CMC sample. (c) Representative TEM image showing precursors of 5 CMC sample. (d) Representative TEM image showing precursors of 10 CMC sample. (e) Representative TEM image showing carbon nanospheres of 1 CMC sample. (f) Representative TEM image showing the carbon nanostructures of 5 CMC sample. (g) Representative TEM image showing carbon nanospheres of 10 CMC sample.

inward shrinkage of the LiCl shell [15]. Unlike the two samples mentioned above, the morphology of the 5 CMC sample deviated from the spherical shape and underwent a greater degree of flattening and stretching. This indicates the coexistence of different morphologies of micelles during the self-assembly process, which include spherical, ellipsoidal and cylindrical shapes (Fig. 1f). The above results visually show that the carbon nanospheres can be tuned from 55 nm to 70 nm by increasing the CMC value of the surfactant from 1 to 10. It shows that the synthesized system has good dynamic tunability.

Next, we investigate the degree of order of the carbon nanomaterials. All three samples have two bands on the primary Raman spectrum, namely the G-band at 1580 cm^{-1} and the D-band at 1350 cm^{-1} (Fig. 2a) [16]. The relatively strong and narrow G-band implies a relatively high degree of graphitization, which is favorable for BS-12 @ LiCl materials. However, the D-band is very broad, which indicates that the sample has an amorphous structure [17]. More importantly, the D-band and G-band of the three samples do not overlap, and the intensity of the G-band is significantly greater than that of the D-band. This further confirms the smaller carbon fraction of graphite lattice defects, edge disorder arrangement and low symmetry structure [18]. In addition to the D and G peaks, a peak called 2D (or G′) peak observed at 2700 cm^{-1} is also prominent in the sample, confirming the presence of graphitic structural carbon in the resulting product [19]. Notably, the computational results show that the I_D/I_G values for 1 CMC, 5 CMC, and 10 CMC are less than 1. This demonstrates the high degree of graphitization of their carbon frameworks [20]. The high L_a value corresponding to the low I_D/I_G value indicates the orderliness of the microcrystal stacking [21]. In addition, further evidence of the degree of graphitization and defects in the BS-12 @ LiCl nanostructures is obtained by using powder X-ray diffraction (XRD). Fig. 2b shows the coexistence of diffraction peaks and diffraction curves for the three sets of samples, indicating the presence of both crystalline and amorphous phase structures in the material [22]. The differences in the characteristic peaks indicate the differences in the crystal structures of the three groups of samples [23]. All three sets of samples show broader (002) diffraction peaks with an asymmetric distribution. This indicates that the BS-12 @ LiCl sample is partially graphitized and contains a certain percentage of defects or amorphous carbon, consistent with the Raman spectroscopy results. Compared to the 1 CMC sample, the d_{002} value calculated according to Bragg's law for the 10 CMC sample is most similar to the layer spacing of ideal graphite ($d_{002} = 0.3354$ nm), showing a more ordered nanocrystalline graphitic carbon. In addition, the graphitization degree g value provides the same information as the d_{002} value. Our research clearly shows that the g values of carbon nanospheres in 10 CMC samples are much higher than those of 1 CMC samples under the same conditions. A comprehensive analysis of these observations suggests that the generated carbon nanospheres are in an intermediate state between the amorphous and crystalline states [24].

The XPS spectra in Fig. 3a provide further information on the composition and structure. The C 1s, O 1s and N 1s peaks can be clearly seen in the XPS spectra, confirming the coexistence of C, O and N in the carbon skeleton. It is noteworthy that the characteristic graphitic carbon peak with a binding energy of about 284.6 eV is present in the spectra of all samples. This provides another piece of supporting evidence for the orderliness of the sample microstructure. The fits of the N 1s and O 1s peaks indicate significant changes in the nitrogen and oxygen contents of the nanocarbon structures. The presence of non-carbon elements indicates a reduced degree of order in the nanocarbon structure. It is worth mentioning that the highest C–C sp^2 peak in the XPS spectrum of the 10 CMC sample indicates the formation of graphitic carbon [25]. In addition, this peak area is the largest, indicating that most of the C elements in the sample are present in the form of graphitic carbon. This is consistent with our previous findings. The high-resolution N 1s spectrum of the 10 CMC sample can be deconvoluted into two peaks at 399.31 and 407.69 eV, corresponding to graphite N and oxidized N, respectively [8,19]. For the O 1s spectrum, the two deconvoluted peaks located at 531.92 and 533.85 eV belong to the C═O and C–O

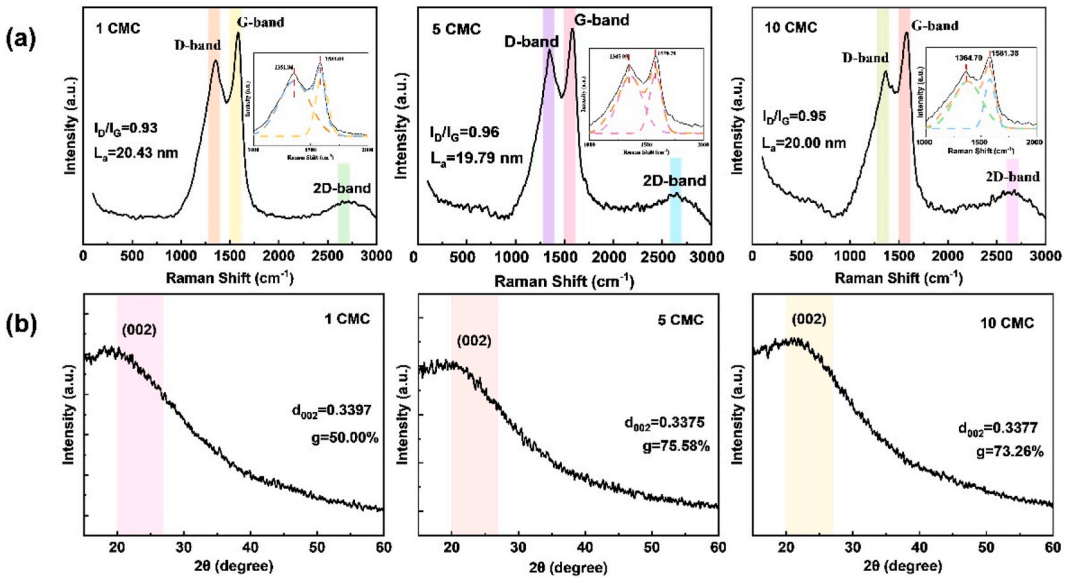

Fig. 2. Degree of graphitization of BS-12 @ LiCl carbon nanostructures. (a) Raman spectra of BS-12 @ LiCl carbon nanostructures. (b) XRD pattern of BS-12 @ LiCl carbon nanostructures.

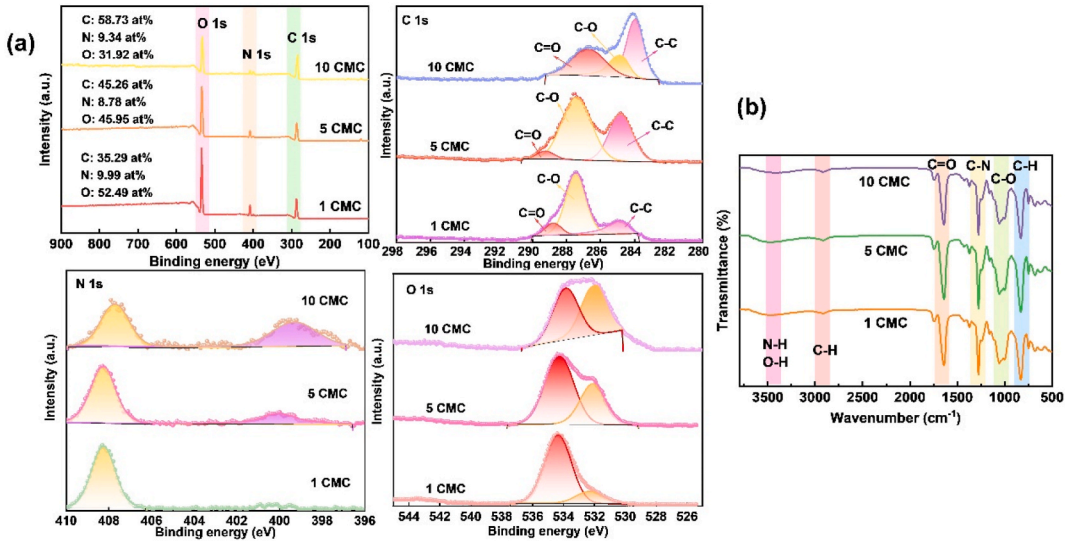

Fig. 3. Elemental composition and surface chemical state of BS-12 @ LiCl carbon nanostructures. (a) XPS spectra of BS-12 @ LiCl carbon nanostructures. (b) FTIR spectra of BS-12 @ LiCl carbon nanostructures.

groups, respectively [10]. To further determine the surface chemical state of the samples, FTIR spectra are obtained (Fig. 3b) and the characteristic peaks of several functional groups are identified. Specifically, the broadband appearing near 3441 cm^{-1} represents the stretching vibration peaks of N–H and O–H [26]. The weak peak near 2919 cm^{-1} is an indicative sign of symmetric and asymmetric stretching of C–H in the CH_2 and CH_3 groups [27]. The strong absorption peak located near 1640 cm^{-1} corresponds to the C═O stretching vibration peak on the surface of the nanocarbon structure [26]. The broad peak near 1275 cm^{-1} is associated with the C–N stretching vibration mode [26]. The peak near 1056 cm^{-1} can be attributed to the stretching vibration of the C–O [28]. The spike near 830.91 cm^{-1} is consistent with the C–H bending vibration pattern [27]. Both XPS and FTIR data show that the samples contain some O and N, which explains well why the BS-12 @ LiCl nanocarbon structure has defects and amorphous carbon structure [29].

Fig. 4a schematically illustrates the formation mechanism of BS-12 @ LiCl carbon nanospheres. At low concentrations, our images clearly detect relatively regular spherical micelles. In fact, when the BS-12 concentration in the system increases from 1 CMC to 5 CMC, the micelles undergo a morphological transformation into spherical, ellipsoidal and cylindrical coexisting structures. It should be noted that the transition from spherical micelles to elongated structures has been shown to occur at small values of the packing parameter (p) [30]. In addition, it has been shown that large amounts of salt can enhance this transformation [30]. Remarkably, the micelles remain

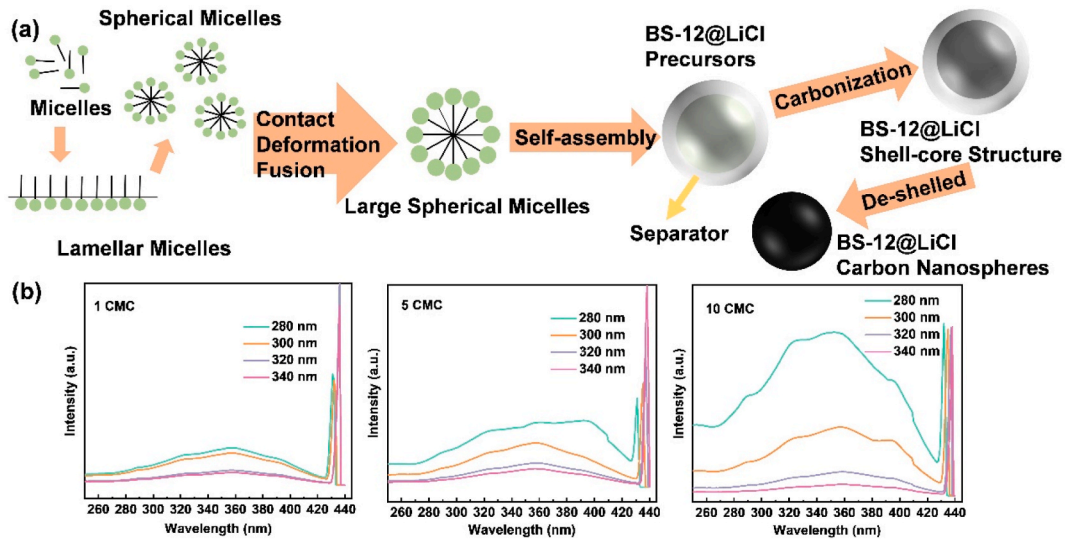

Fig. 4. Growth mechanism and luminescence properties of BS-12 @ LiCl carbon nanostructures. (a) Schematic diagram of the formation mechanism of BS-12 @ LiCl carbon nanospheres. (b) Excitation-dependent PL spectra of BS-12 @ LiCl when the excitation wavelength is varied in the range of 280~340 nm.

spherical when the BS-12 concentration in the system is increased to 10 CMC. However, we observe a further expansion of its morphology, which leads to a further increase in size. Thus, by controlling the concentration of BS-12, the micelle size can be precisely and dynamically controlled. When the concentration is low, lamellar micelles appear and gradually assemble continuously into spherical micelles. When the concentration is further increased, the spherical micelles undergo contact, deformation, and fusion as the assembly proceeds. The small spheres evolve into cylindrical or large spheres [14]. After carbonization, the salt-coated BS-12 @ LiCl precursors can be easily converted into carbon nanospheres with a shell-core structure. In other words, the dynamic nature of the micellar system allows for intelligent assembly, which is highly dependent on the concentration of BS-12.

When comparing the synthesized carbon nanospheres with those prepared by other researchers using innovative strategies in recent years, it is shown that our proposed strategy is a robust method for the facile synthesis of carbon nanospheres with tunable sizes below 100 nm as well as high nitrogen content. With respect to adjustable size, J. Jeskey et al. proposed an EDTA-assisted method for the preparation of carbon nanospheres with adjustable sizes ranging from 100 to 375 nm [31]. We have demonstrated that carbon nanospheres with tunable diameters below 100 nm can be successfully synthesized using the BS-12 @ LiCl self-assembly strategy. The comparison of the two results highlights the advantages of our proposed strategy. With respect to nitrogen content, Y. Qiu et al. developed a one-step direct template method and unique pyrolysis procedure to synthesize N-doped carbon nanospheres with a nitrogen content of 4.17 at% [32]. Fig. 3a has demonstrated that our synthesized carbon nanospheres contain nitrogen up to 8.78–9.99 at % and do not require an additional nitrogen source.

Finally, to better understand the luminescence properties of BS-12 @ LiCl nanocarbon structures, we obtained the PL spectra of the samples after excitation at different wavelengths (Fig. 4b). Interestingly, when the excitation wavelength is increased from 280 nm to 340 nm, a unique bimodal PL emission behavior can be seen for the three groups of samples [33]. In addition, the maximum emission peaks of the samples are all concentrated around 360 nm and 430 nm, indicating that the samples have UV luminescent properties [34]. In general, UV luminescence is attributed to the direct recombination of band-edge excitons. Indeed, the presence of excitons is closely related to the crystalline state of carbon nanostructures. The greater the degree of crystallinity of the sample, the more favorable it is in the presence of excitons. The significant enhancement of the UV peaks of the 10 CMC sample further corroborates that this sample has the most complete crystallization and the highest degree of graphitization. Unlike most of the previously reported carbon nanostructures, the position of the emission peaks of the BS-12 @ LiCl carbon nanostructures remains almost unchanged. This indicates that the size of the prepared carbon nanospheres is relatively uniform, so there is no "fluorescence resonance energy transfer" between the nanospheres, resulting in the luminescence peaks not being shifted due to the change of the excitation wavelength. Based on the above analysis, the BS-12 @ NaCl carbon nanospheres have good photoluminescence properties in the violet wavelength band. In addition, we deduce that due to the presence of N and O atoms, the positions of functional groups on the surface of BS-12 @ LiCl carbon nanostructures can act as energy-trapping sites capable of trapping excitons and undergoing leaps to generate fluorescence [35]. These results predict that BS-12 @ NaCl carbon nanospheres are expected to be applied in the field of UV light-emitting devices.

4. Conclusions

In conclusion, carbon nanospheres with tunable size and specific fluorescence properties are intelligently synthesized by the BS-12 @ LiCl self-assembly method. This method differs from traditional synthesis methods in that it is characterized by the introduction of the concept of "separator". The synthesis process involves the formation of a dynamically stable micellar system to guide the self-assembly of the core (BS-12) and shell (LiCl) into BS-12 @ LiCl precursors. This method differs from conventional synthesis methods in that it introduces the concept of a "separator" (LiCl), which makes the synthesis cheaper, simpler, and more environmentally friendly. Specifically, LiCl plays a key role in the formation of the core and shell in one step, as well as in the protection of the original skeleton of the carbide unchanged. Even more exciting, LiCl can be easily recovered through the crystallization process. Impressively, the results of TEM investigations show the ability to adjust the size of carbon nanospheres by varying the concentrations of BS-12. The obtained carbon nanospheres are tunable from 55 to 70 nm. Raman and XRD show certain defects in the structure. XPS and FTIR data indicate that the carbon nanospheres have a percentage of N and O content, which further explains the defects. The formation mechanism of carbon nanospheres further demonstrates that micelle morphology and size can be tuned on demand by simply adjusting the concentration of surfactant, resulting in controllable carbon nanostructures and sizes. PL analysis shows that carbon nanospheres have specific optical properties (UV luminescence). We envision that this surfactant @ salt self-assembly method may open new opportunities for the synthesis of novel nanocarbon structures. These nanocarbons will lead to new areas and applications related to their unforeseen properties and functions.

CRediT authorship contribution statement

Bingxuan Du: Writing – original draft, Investigation, Formal analysis. **Haichao Li:** Supervision, Methodology, Funding acquisition, Conceptualization. **Conglin Zhang:** Visualization, Data curation. **Qingsong Ji:** Visualization, Data curation.

Declaration of competing interest

We declare that we have no financial and personal relationships with other people or organizations that can inappropriately influence our work, there is no professional or other personal interest of any nature or kind in any product, service and/or company that could be construed as influencing the position presented in, or the review of, the manuscript entitled.

Acknowledgements

This work was supported by Carbon Peaking and Carbon Neutrality Research Projects of Qinghai Minzu University (CPCT202301).

References

[1] K. Itami, T. Maekawa, Molecular nanocarbon science: present and future, Nano Lett. 20 (2020) 4718–4720, https://doi.org/10.1021/acs.nanolett.0c02143.
[2] X. Du, C.X. Zhao, M.Y. Zhou, T.Y. Ma, H.W. Huang, M. Jaroniec, X.J. Zhang, S.Z. Qiao, Hollow carbon nanospheres with tunable hierarchical pores for drug, gene, and photothermal synergistic treatment, Small 13 (2017) 1602592, https://doi.org/10.1002/smll.201602592.
[3] M. Sirignano, C. Russo, A. Ciajolo, One-step synthesis of carbon nanoparticles and yellow to blue fluorescent nanocarbons in flame reactors, Carbon 156 (2020) 370–377, https://doi.org/10.1016/j.carbon.2019.09.068.
[4] Q.G. Wang, L. He, L.Y. Zhao, R.S. Liu, W.P. Zhang, A.H. Lu, Surface charge-driven nanoengineering of monodisperse carbon nanospheres with tunable surface roughness, Adv. Funct. Mater. 30 (2020) 1906117, https://doi.org/10.1002/adfm.201906117.
[5] N. Díez, M. Sevilla, A.B. Fuertes, Dense (non-hollow) carbon nanospheres: synthesis and electrochemical energy applications, Materials Today Nano 16 (2021) 100147, https://doi.org/10.1016/j.mtnano.2021.100147.
[6] J.Y. Piao, D.S. Bin, S.Y. Duan, X.J. Lin, D. Zhang, A.M. Cao, A facile template free synthesis of porous carbon nanospheres with high capacitive performance, Sci. China Chem. 61 (2018) 538–544, https://doi.org/10.1007/s11426-017-9181-9.
[7] S.G. Gao, L. Zhang, H.T. Yu, H.Q. Wang, Z.W. He, K. Huang, Palladium-encapsulated hollow porous carbon nanospheres as nanoreactors for highly efficient and size-selective catalysis, Carbon 175 (2021) 307–311, https://doi.org/10.1016/j.carbon.2021.01.023.
[8] Y.T. Qiu, M.Z. Hou, J.C. Gao, H.L. Zhai, H.M. Liu, M.M. Jin, X. Liu, L.F. Lai, One-step synthesis of monodispersed mesoporous carbon nanospheres for high-performance flexible quasi-solid-state micro- supercapacitors, Small 15 (2019) 1903836, https://doi.org/10.1002/smll.201903836.
[9] H.Y. Zhao, F. Zhang, S.M. Zhang, S.G. He, F. Shen, X.G. Han, Y.D. Yin, C.B. Gao, Scalable synthesis of sub-100 nm hollow carbon nanospheres for energy storage applications, Nano Res. 11 (2018) 1822–1833, https://doi.org/10.1007/s12274-017-1800-3.
[10] D.Y. Guo, Y.B. Fu, F.X. Bu, H.C. Liang, L.L. Duan, Z.W. Zhao, C.Y. Wang, A.M. El-Toni, W. Li, D.Y. Zhao, Monodisperse ultrahigh nitrogen-containing mesoporous carbon nanospheres from melamine-formaldehyde resin, Small Methods 5 (2021) 2001137, https://doi.org/10.1002/smtd.202001137.
[11] G.H. Wang, K. Chen, J. Engelhardt, H. Tüysüz, H.J. Bongard, W. Schmidt, F. Schüth, Scalable one-pot synthesis of yolk–shell carbon nanospheres with yolk-supported Pd nanoparticles for size-selective catalysis, Chem. Mater. 30 (2018) 2483–2487, https://doi.org/10.1021/acs.chemmater.8b00456.
[12] F. Dehghani, S. Shahmoradi, M. Naghizadeh, T. Firuzyar, A. Vaez, S.R. Kasaee, A.M. Amani, S. Mosleh-Shiraz, Magnetic graphite-ODA @ $CoFe_2O_4$: attempting to produce and characterize the development of an innovative nanocomposite to investigate its antimicrobial properties, Appl. Phys. A 128 (2022) 1–13, https://doi.org/10.1007/s00339-022-05387-2.
[13] A. Mirzaei, W. Oum, H. Ham, Y.J. Kwon, S. Mosleh-Shirazi, K.Y. Shin, D.J. Yu, S.W. Kang, E.B. Kim, S.S. Kim, H.W. Kim, Catalyst and substrate-free synthesis of graphene nanosheets by unzipping C60 fullerene clusters using a pulse current method, Mater. Sci. Semicond. Process. 149 (2022) 106831, https://doi.org/10.1016/j.mssp.2022.106831.
[14] L. Peng, H.R. Peng, C.-T. Hung, D.Y. Guo, L.L. Duan, B. Ma, L.L. Liu, W. Li, D.Y. Zhao, Programmable synthesis of radially gradient-structured mesoporous carbon nanospheres with tunable core-shell architectures, Chem 7 (2021) 1020–1032, https://doi.org/10.1016/j.chempr.2021.01.001.
[15] R.L. Cai, Y.S. Si, B. You, M. Chen, L.M. Wu, Yolk–shell carbon nanospheres with controlled structure and composition by self-activation and air activation, ACS Appl. Mater. Interfaces 12 (2020) 28738–28749, https://doi.org/10.1021/acsami.0c02980.
[16] Z.L. Li, L.B. Deng, L.A. Kinloch, R.J. Young, Raman spectroscopy of carbon materials and their composites: graphene, nanotubes and fibres, Prog. Mater. Sci. 135 (2023) 101089, https://doi.org/10.1016/j.pmatsci.2023.101089.
[17] G. Wang, X.Y. Pan, J.N. Kumar, Y. Liu, One-step synthesis of hollow carbon nanospheres in non-coordinating solvent, Carbon 83 (2015) 180–182, https://doi.org/10.1016/j.carbon.2014.11.045.
[18] J.R. Zhang, X. Wang, G.C. Qi, B.H. Li, Z.H. Song, H.B. Jiang, X.H. Zhang, J.L. Qiao, A novel N-doped porous carbon microsphere composed of hollow carbon nanospheres, Carbon 96 (2016) 864–870, https://doi.org/10.1016/j.carbon.2015.10.045.
[19] Z.Y. Pang, G.S. Li, X.L. Zou, C.T. Sun, C.H. Hu, W. Tang, L. Ji, H.Y. Hsu, Q. Xu, X.G. Lu, An integrated strategy towards the facile synthesis of core-shell SiC-derived carbon@N-doped carbon for high-performance supercapacitors, J. Energy Chem. 56 (2021) 512–521, https://doi.org/10.1016/j.jechem.2020.08.042.
[20] C. Zhou, S. Geng, X.W. Xu, T.H. Wang, L.Q. Zhang, X.J. Tian, F. Yang, H.T. Yang, Y.F. Li, Lightweight hollow carbon nanospheres with tunable sizes towards enhancement in microwave absorption, Carbon 108 (2016) 234–241, https://doi.org/10.1016/j.carbon.2016.07.015.
[21] X. Ge, C. Klingshirn, M. Morales, M. Wuttig, O. Rabin, S. Zhang, L.G. Salamanca-Riba, Electrical and structural characterization of nano-carbon–aluminum composites fabricated by electro-charging-assisted process, Carbon 173 (2021) 115–125, https://doi.org/10.1016/j.carbon.2020.10.063.
[22] H.X. Liang, R.R. Sun, B. Song, Q.Q. Sun, P. Peng, D. She, Preparation of nitrogen-doped porous carbon material by a hydrothermal-activation two-step method and its high-efficiency adsorption of Cr(VI), J. Hazard Mater. 387 (2020) 121987, https://doi.org/10.1016/j.jhazmat.2019.121987.
[23] H.X. Liang, B. Song, P. Peng, G.J. Jiao, X. Yan, D. She, Preparation of three-dimensional honeycomb carbon materials and their adsorption of Cr(VI), Chem. Eng. J. 367 (2019) 9–16, https://doi.org/10.1016/j.cej.2019.02.121.
[24] X.J. Chen, Y.X. Guo, J.L. Cui, H.R. Zhang, F.Q. Cheng, Y. Zou, Activated carbon preparation with the addition of coke-making by-product-coke powder: texture evolution and mechanism, J. Clean. Prod. 237 (2019) 117812, https://doi.org/10.1016/j.jclepro.2019.117812.
[25] G.D. Park, J.H. Kim, Y.C. Kang, General strategy for yolk-shell nanospheres with tunable compositions by applying hollow carbon nanospheres, Chem. Eng. J. 406 (2021) 126840, https://doi.org/10.1016/j.cej.2020.126840.
[26] Y.F. Zhang, F.P. Du, L. Chen, W.C. Law, C.Y. Tang, Synthesis of deformable hydrogel composites based on Janus bilayer multi-walled carbon nanotubes/host-guest complex structure, Compos. B Eng. 164 (2019) 121–128, https://doi.org/10.1016/j.compositesb.2018.11.068.
[27] M. Varga, T. Izak, V. Vretenar, H. Kozak, J. Holovsky, A. Artemenko, M. Hulman, V. Skakalova, D.S. Lee, A. Kromka, Diamond/carbon nanotube composites: Raman, FTIR and XPS spectroscopic studies, Carbon 111 (2017) 54–61, https://doi.org/10.1016/j.carbon.2016.09.064.
[28] C. Yang, Z.W. Li, Y. Huang, K.Y. Wang, Y.Z. Long, Z.L. Guo, X.Y. Li, H. Wu, Continuous roll-to-roll production of carbon nanoparticles from candle soot, Nano Lett. 21 (2021) 3198–3204, https://doi.org/10.1021/acs.nanolett.1c00452.
[29] J. Zhang, J.J. Zhang, F. He, Y.J. Chen, J.W. Zhu, D.L. Wang, S.C. Mu, H.Y. Yang, Defect and doping Co-engineered non-metal nanocarbon ORR electrocatalyst, Nano-Micro Lett. 13 (2021) 65, https://doi.org/10.1007/s40820-020-00579-y.
[30] K. Schäfer, H.B. Kolli, M.K. Christensen, S.L. Bore, G. Diezemann, J. Gauss, G. Milano, R. Lund, M. Cascella, Supramolecular packing drives morphological transition of charged surfactant micelles, Angew. Chem. Int. Ed. 59 (2020) 18591, https://doi.org/10.1002/anie.202004522.
[31] J. Jeskey, Y. Chen, S. Kim, Y. Xia, EDTA-assisted synthesis of nitrogen-doped carbon nanospheres with uniform sizes for photonic and electrocatalytic applications, Chem. Mater. 35 (2023) 3024–3032, https://doi.org/10.1021/acs.chemmater.3c00341.
[32] Y. Qiu, M. Hou, J. Gao, H. Zhai, H. Liu, M. Jin, X. Liu, L. Lai, One-step synthesis of monodispersed mesoporous carbon nanospheres for high-performance flexible quasi-solid-state micro-supercapacitors, Small 15 (2019) 1903836, https://doi.org/10.1002/smll.201903836.
[33] Q.Q. Ran, X.P. Wang, P. Ling, P.W. Yan, J. Xu, L. Jiang, Y. Wang, S. Su, S. Hu, J. Xiang, A thermal-assisted electrochemical strategy to synthesize carbon dots with bimodal photoluminescence emission, Carbon 193 (2022) 404–411, https://doi.org/10.1016/j.carbon.2022.03.041.
[34] P. Yang, Z.Q. Zhu, T. Zhang, M.Z. Chen, Y.Z. Cao, W. Zhang, X. Wang, X.Y. Zhou, W.M. Chen, Facile synthesis and photoluminescence mechanism of green emitting xylose-derived carbon dots for anti-counterfeit printing, Carbon 146 (2019) 636–649, https://doi.org/10.1016/j.carbon.2019.02.028.
[35] P. Reineck, D.W.M. Lau, E.R. Wilson, K. Fox, M.R. Field, C. Deeleepojananan, V.N. Mochalin, B.C. Gibson, Effect of surface chemistry on the fluorescence of detonation nanodiamonds, ACS Nano 11 (2017) 10924–10934, https://doi.org/10.1021/acsnano.7b04647.